Ultra-low power parametric frequency conversion in a silicon microring resonator

Amy C. Turner,[1] Mark A. Foster,[2] Alexander L. Gaeta,[2] and Michal Lipson[1*]

[1]*School of Electrical and Computer Engineering, Cornell University, Ithaca, NY 14853, USA*
[2]*School of Applied and Engineering Physics, Cornell University, Ithaca, NY 14853, USA*
**Corresponding author: lipson@ece.cornell.edu*

Abstract: We demonstrate parametric wavelength conversion via four-wave mixing using ultra-low peak pump powers of a few milliwatts in a micrometer-scale silicon device. The response time of our device is 100 ps allowing for implementation in high-bandwidth optical communications. At these ultra-low power levels and microscale sizes, it should be possible to realize hundreds of these devices operating simultaneously on a single chip.

© 2008 Optical Society of America

OCIS codes: (190.4390) Nonlinear optics, integrated optics; (130.7405) Wavelength conversion devices.

References and links

1. G. P. Agrawal, *Nonlinear Fiber Optics* (Academic Press, New York, 2001).
2. K. Kikuchi and C. Lorattanasane, "Design of Highly Efficient Four-Wave Mixing Devices Using Optical Fibers," IEEE Photon. Technol. Lett. **6**, 992-994 (1994).
3. I. H. Agha, Y. Okawachi, M. A. Foster, J. E. Sharping, and A. L. Gaeta, "Four-wave mixing parametric oscillations in dispersion-compensated high-Q optical microspheres," Phys. Rev. A **76**, 043837 (2007).
4. T. J. Kippenberg, S. M. Spillane, and K. J. Vahala, "Kerr-nonlinearity optical parametric oscillation in an ultrahigh-Q toroid microcavity," Phys. Rev. Lett. **93**, 083904 (2004).
5. M. A. Foster, A. C. Turner, J. E. Sharping, B. S. Schmidt, M. Lipson and A. L. Gaeta, "Broad-band optical parametric gain on a silicon photonic chip," Nature **441**, 960-963 (2006).
6. R. L. Espinola, J. I. Dadap, R. M. Osgood, S. J. McNab, and Y. A. Vlasov, "C-band wavelength conversion in silicon photonic wire waveguides," Opt. Express **13**, 4341-4349 (2005) http://www.opticsinfobase.org/abstract.cfm?URI=oe-13-11-4341.
7. M. A. Foster, A. C. Turner, R. Salem, M. Lipson, and A. L. Gaeta, "Broad-band continuous-wave parametric wavelength conversion in silicon nanowaveguides," Opt. Express **15**, 12949-12958 (2007) http://www.opticsinfobase.org/abstract.cfm?URI=oe-15-20-12949.
8. H. Fukuda, K. Yamada, T. Shoji, M. Takahashi, T. Tsuchizawa, T. Watanabe, J. -i. Takahashi, and S. -i. Itabashi, "Four-wave mixing in silicon wire waveguides," Opt. Express **13**, 4629-4637 (2005) http://www.opticsinfobase.org/abstract.cfm?URI=oe-13-12-4629.
9. Y. -H. Kuo, H. Rong, V. Sih, S. Xu, M. Paniccia, and O. Cohen, "Demonstration of wavelength conversion at 40 Gb/s data rate in silicon waveguides," Opt. Express **14**, 11721-11726 (2006) http://www.opticsinfobase.org/abstract.cfm?URI=oe-14-24-11721.
10. H. Rong, Y. -H. Kuo, A. Liu, M. Paniccia, and O. Cohen, "High efficiency wavelength conversion of 10 Gb/s data in silicon waveguides," Opt. Express **14**, 1182-1188 (2006) http://www.opticsinfobase.org/abstract.cfm?URI=oe-14-3-1182.
11. K. Yamada, H. Fukuda, T. Tsuchizawa, T. Watanabe, T. Shoji, and S. Itabashi, "All-optical efficient wavelength conversion using silicon photonic wire waveguide," IEEE Photon. Technol. Lett. **18**, 1046-1048 (2006).
12. R. Salem, M. A. Foster, A. C. Turner, D. F. Geraghty, M. Lipson and A. L. Gaeta, "Signal regeneration using low-power four-wave mixing on silicon chip," Nature Photon. **2**, 35-38 (2007).
13. S. Ayotte, H. Rong, S. Xu, O. Cohen, and M. J. Paniccia, "Multichannel dispersion compensation using a silicon waveguide-based optical phase conjugator," Opt. Lett. **32**, 2393-2395 (2007) http://www.opticsinfobase.org/abstract.cfm?URI=ol-32-16-2393.
14. S. Ayotte, S. Xu, H. Rong, O. Cohen, and M. J. Paniccia, "Dispersion compensation by optical phase conjugation in silicon waveguide," Electron. Lett. **43**, 1037-1039 (2007).
15. A. Ashkin, G. Boyd, and J. Dziedzic, "Resonant optical second harmonic generation and mixing," IEEE J. Quantum Electron. **2**, 109-124 (1966).
16. V. R. Almeida, C. A. Barrios, R. R. Panepucci, and M. Lipson, "All-optical control of light on a silicon chip," Nature **431**, 1081-1084 (2004).

#92476 - $15.00 USD Received 4 Feb 2008; revised 19 Mar 2008; accepted 19 Mar 2008; published 26 Mar 2008

17. V. R. Almeida, C. A. Barrios, R. R. Panepucci, M. Lipson, M. A. Foster, D. G. Ouzounov, and A. L. Gaeta, "All-optical switching on a silicon chip," Opt. Lett. **29**, 2867-2869 (2004) http://www.opticsinfobase.org/abstract.cfm?URI=ol-29-24-2867.
18. Q. Xu, B. Schmidt, S. Pradhan, and M. Lipson, "Micrometre-scale silicon electro-optic modulator," Nature **435**, 325-327 (2005).
19. P. Dong, S. F. Preble, and M. Lipson, "All-optical compact silicon comb switch," Opt. Express **15**, 9600-9605 (2007) http://www.opticsinfobase.org/abstract.cfm?URI=oe-15-15-9600.
20. Q. Xu, B. Schmidt, J. Shakya, and M. Lipson, "Cascaded silicon micro-ring modulators for WDM optical interconnection," Opt. Express **14**, 9430-9435 (2006) http://www.opticsinfobase.org/abstract.cfm?URI=oe-14-20-9431.
21. B. E. Little, J. S. Foresi, G. Steinmeyer, E. R. Thoen, S. T. Chu, H. A. Haus, E. P. Ippen, L. C. Kimerling, and W. Greene, "Ultra-compact Si-SiO_2 microring resonator optical channel dropping filters," IEEE Photon. Technol. Lett. **10**, 549-551 (1998).
22. M. Cai, O. Painter, and K. Vahala, "Observation of Critical Coupling in a Fiber Taper to a Silica-Microsphere Whispering-Gallery Mode System," Phys. Rev. Lett. **85**, 74-77 (2000).
23. A. C. Turner, C. Manolatou, B. S. Schmidt, M. Lipson, M. A. Foster, J. E. Sharping, and A. L. Gaeta, "Tailored anomalous group-velocity dispersion in silicon channel waveguides," Opt. Express **14**, 4357-4362 (2006) http://www.opticsinfobase.org/abstract.cfm?URI=oe-14-10-4357.
24. M. Borselli, T. J. Johnson, and O. Painter, "Accurate measurement of scattering and absorption loss in microphotonic devices," Opt. Lett. **32**, 2954-2956 (2007) http://www.opticsinfobase.org/abstract.cfm?URI=ol-32-20-2954.
25. P. P. Absil, J. V. Hryniewicz, B. E. Little, P. S. Cho, R. A. Wilson, L. G. Joneckis, and P. -T. Ho, "Wavelength conversion in GaAs mirco-ring resonators," Opt. Lett. **25**, 554-556 (2000) http://www.opticsinfobase.org/abstract.cfm?URI=ol-25-8-554.
26. P. Del'Haye, A. Schliesser, O. Arcizet, T. Wilken, R. Holzwarth and T. J. Kippenberg, "Optical frequency comb generation from a monolithic microresonator," Nature **450**, 1214-1217 (2007).
27. B. G. Lee, B. A. Small, K. Bergman, Q. Xu, and M. Lipson, "Transmission of high-data-rate optical signals through a micrometer-scale silicon ring resonator," Opt. Lett. **31**, 2701-2703 (2006) http://www.opticsinfobase.org/abstract.cfm?URI=ol-31-18-2701.
28. R. A. Soref, and B. R. Bennett, "Electrooptical effects in silicon," IEEE J. Quantum Electron. **QE-23**, 123–129 (1987).
29. A. D. Bristow, N. Rotenberg, and H. M. van Driel, "Two-photon absorption and Kerr coefficients of silicon for 850-2200 nm," Appl. Phys. Lett. **90**, 191104 (2007).
30. M. A. Foster and A. L. Gaeta, "Wavelength Dependence of the Ultrafast Third-Order Nonlinearity of Silicon," in *Conference on Lasers and Electro-Optics/Quantum Electronics and Laser Science Conference and Photonic Applications Systems Technologies*, OSA Technical Digest Series (CD) (Optical Society of America, 2007), paper CTuY5. http://www.opticsinfobase.org/abstract.cfm?URI=CLEO-2007-CTuY5
31. H. K. Tsang, C. S. Wong, T. K. Liang, I. E. Day, S. W. Roberts, A. Harpin, J. Drake, and M. Asghari, "Optical dispersion, two-photon absorption and self-phase modulation in silicon waveguides at 1.5 μm wavelength," Appl. Phys. Lett. **80**, 416-418 (2002).
32. S. F. Preble, Q. Xu, B. S. Schmidt, and M. Lipson, "Ultrafast all-optical modulation on a silicon chip," Opt. Lett. **30**, 2891-2893 (2005) http://www.opticsinfobase.org/abstract.cfm?URI=ol-30-21-2891.

1. Introduction

Traditionally nonlinear optical processes in solid state devices such as amplification, switching and wavelength conversion require relatively high powers for operation, which limits the prospect of their miniaturization and integration on-chip [1]. Here we demonstrate four-wave mixing (FWM), a nonlinear process used in high bandwidth optical communications, using ultra-low powers in a chip-scale device. FWM devices operating at low peak powers around 20-30 mW have been demonstrated by using extremely long lengths (11.4 km) of optical fiber [2]. Also, parametric processes using even lower pump powers (a few 100 μW) have been observed in silica glass microspheres and microtoroids, however the extremely high quality factors limit their response times to approximately 100 ns [3, 4]. In silicon, the nonlinear process of FWM has been demonstrated for parametric amplification [5], wavelength conversion [6-11], signal regeneration [12], and optical phase conjugation [13, 14], and is implemented using centimeter-scale devices which require peak powers on the order of 100 mW for operation. By combining the high transverse optical confinement of silicon nanowaveguides with resonant enhancement from a silicon microresonator, we demonstrate ultra-low power FWM in a micron-scale device requiring only a few milliwatts

#92476 - $15.00 USD Received 4 Feb 2008; revised 19 Mar 2008; accepted 19 Mar 2008; published 26 Mar 2008
(C) 2008 OSA

of peak pump power. Our devices are capable of response times of 100 ps, making them feasible for use in high-bandwidth optical communications.

Since FWM is a nonlinear process, it is by definition a function of the optical intensity. The platform we use in order to increase the optical intensity in the nonlinear medium consists of a micro-scale photonic structure that confines light both in the transverse and longitudinal direction. The structures are based on silicon nanowaveguides with high transverse confinement due to the strong index contrast between the silicon core and the SiO_2 cladding. To further enhance the efficiency, microcavities are used for longitudinal confinement [15]. The microcavities used here are ring resonators which have been critical in the demonstration of low-power and small-footprint photonic devices such as modulators [16-18], switches [19] and filters [20, 21]. The rings resonators have radii of 50-μm and 10-μm (shown in Fig. 1). The transmission of the 50-μm-radius structure is shown as the upper plot (blue) in Fig. 2 with a free-spectral range of 1.6 nm and exhibits a resonance quality factor $Q = \lambda/\Delta\lambda = 19{,}000$ at the center wavelength of 1550 nm. Although not apparent in the figure due to sample spacing, the measured extinction ratio for this resonance is greater than 15 dB, which indicates that we are operating close to critical coupling where all of the power in the input waveguide is coupled to and circulates within the ring [22]. The free spectral range and quality factor of the 10-μm-ring are 8 nm and 23,000, respectively.

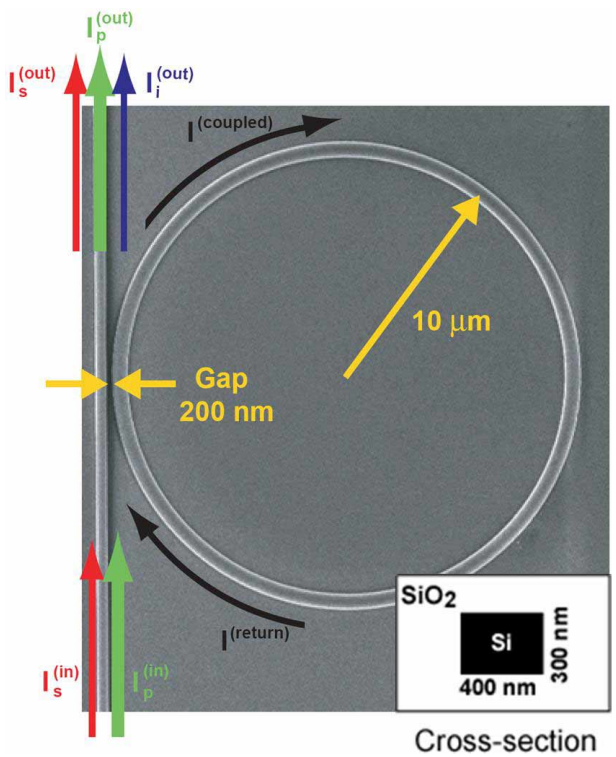

Fig. 1. The microring resonator, shown in this SEM prior to being clad, is used for performing the parametric nonlinear optical process of four-wave mixing. Here we demonstrate low-power frequency conversion of an input signal, $I_s^{(in)}$, to an output idler, $I_i^{(out)}$. Inset: Schematic of cross-section of waveguide.

2. Experiment

In order to demonstrate ultra-low power FWM we use the aforementioned silicon photonic ring resonators and observe a strong enhancement of the nonlinear process due to the optical resonance. The cross-sectional dimensions of the waveguides (300-nm height and 400-nm width) provide an anomalous group-velocity dispersion (GVD) value of 1600 ps/(nm·km)

#92476 - $15.00 USD Received 4 Feb 2008; revised 19 Mar 2008; accepted 19 Mar 2008; published 26 Mar 2008
(C) 2008 OSA

near the pump wavelength of 1550 nm. This allows for wavelength conversion over a bandwidth of more than 50 nm [7, 23].

A tapered lens fiber with a fiber polarization controller to optimize the TE-like mode is aligned to the inverse taper mode converter in the silicon waveguide, allowing for coupling into the waveguide. The pump wavelength is centered on a resonance of the ring (e.g. at 1550 nm for the 50-µm-radius ring), and the signal is scanned across the C-band (see main part of Fig. 2). The output of the waveguide is collimated, sent through a polarizing filter, coupled into a fiber, and sent to an optical spectrum analyzer (OSA). The structures are fabricated on a silicon-on-insulator (SOI) substrate with a 3-µm buried oxide and a 1-µm plasma enhanced chemical vapor deposition (PECVD) oxide cladding. The bus waveguide loss is about 3 dB/cm due to stitching errors from the electron beam lithography, scattering losses from roughness and absorption due to surface states [24]. We define the conversion efficiency as the ratio of the output idler, $I_i^{(out)}$, to the input signal, $I_s^{(in)}$ (Fig. 1 and Eq. (1)) [25]. Experimentally, this value is determined by removing contributions from the input coupling into the waveguide (5 dB), propagation losses in the bus waveguide before and after the ring (3 dB/cm) and coupling losses out of the waveguide as the light is sent through the collimator and into the optical spectrum analyzer (5 dB).

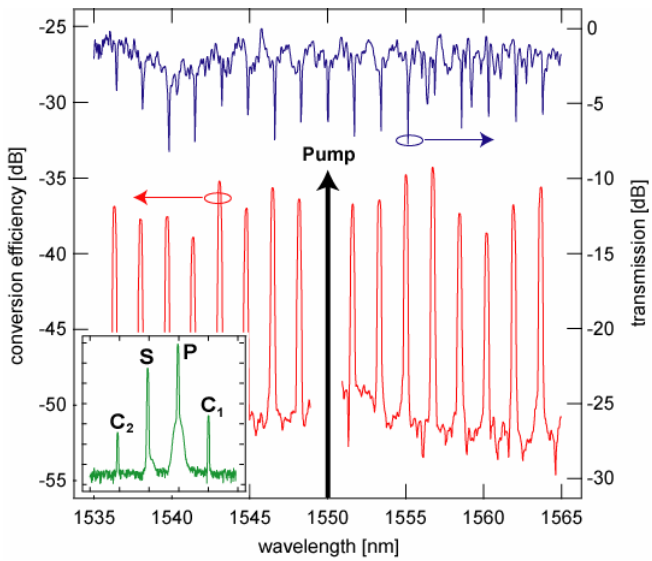

Fig. 2. Measured conversion efficiency as a function of wavelength for several ring resonances (red) and transmission spectrum (blue) in a 50-µm radius ring. A 15-dB enhancement of the FWM process due to the resonant cavity is observed. Inset: Sample on-resonance FWM spectrum with pump (P), signal (S), converted idler of interest (C_1), and additional converted idler (C_2).

An example of a FWM spectrum is shown as the inset of Fig. 2. The pump is tuned to one cavity resonance at 1550 nm, and the input signal is tuned to a different cavity resonance at 1544 nm. Since the resonators are not ultra-high *Q*, feedback-based locking to the resonance is not required to maintain FWM. As seen in the inset of Fig. 2, two converted idlers are observed in this spectrum (C_1 and C_2) and it is the converted idler closer to the pump (C_1) that is of interest in this investigation. With increased conversion efficiency and parametric amplification, additional converted idlers (such as C_2) can potentially yield an on-chip optical frequency comb [26]. The coupled pump and signal powers in the bus waveguide before the ring are 5 mW and 100 µW, respectively. In order to observe the conversion spectrum as seen in the red curve of the main part of Fig. 2, we keep the pump tuned to the cavity resonance at 1550 nm while we scan the input signal across the C-band and measure the conversion

#92476 - $15.00 USD Received 4 Feb 2008; revised 19 Mar 2008; accepted 19 Mar 2008; published 26 Mar 2008
(C) 2008 OSA

efficiency to the idler. As shown by the red curve in Fig. 2, the conversion of the idler is increased by ~15 dB when both the pump and the signal wavelengths are tuned to resonances of the ring as compared to when the signal is off-resonance. This verifies that frequency conversion is occurring in the ring. Conversion is observed over a span greater than 30 nm and is limited by the tunable filters used in our experimental setup. Note that the time scale of the operation of the device is limited by the bandwidth of the resonator. The devices demonstrated here can be used for optical data rates as high as 10 Gbit/s [27].

We measure the FWM efficiency as a function of input pump power for the 10-μm and 50-μm radius ring resonators, and both the experiment and the theoretical model are plotted in Fig. 3. Using a pump power of 1 mW and an input signal power of 100 μW before the 10-μm radius ring (Fig. 3(a)), the power of the converted signal, or idler, coupled back into the bus waveguide from the ring is 100 nW, indicating a net conversion efficiency from the input signal to converted output of about -30 dB. Using the 50-μm radius ring we observe a peak conversion efficiency of -25.4 dB with only 11.3 mW of CW pump power and 100 μW of signal power before the ring (Fig. 3(b)). The increased conversion efficiency in the rings is due to the pump and signal intensity buildup within the resonator and is limited mainly by the absorption of light due to the presence of free carriers that are generated in the structures. A reduction of the size of the device from a ring with radius of 50 μm to 10 μm correspondingly reduces the power requirements of the devices due to the smaller mode volume; however, the conversion efficiencies in the 10-μm-ring are not as large as those achieved in the larger ring since the free carriers build up faster in the smaller volume which results in increased loss. Furthermore, in straight waveguides, higher conversion efficiencies can be achieved (-9.6 dB) due to reduced free-carrier buildup in the large device, however this requires more than 100 mW of pump power [7].

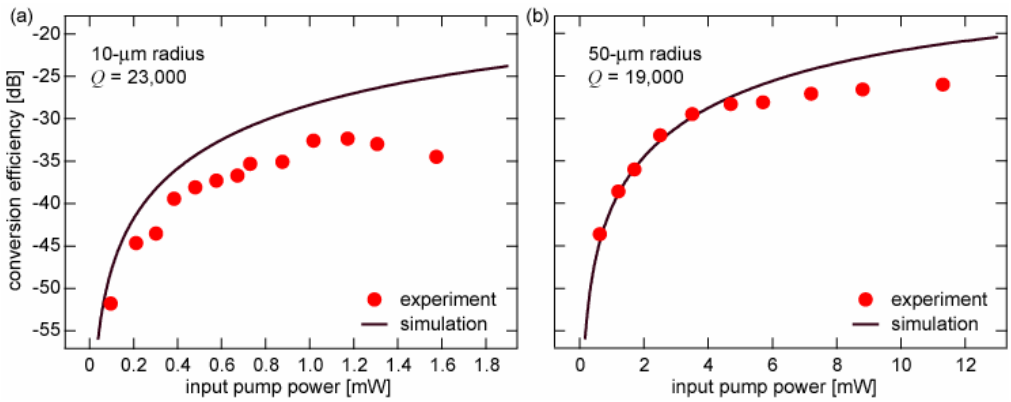

Fig. 3. Simulated (-) and experimental (●) conversion efficiency as a function of input pump power for rings with free carrier lifetime of 500 ps, (a) 10-μm radius and a *Q* of 23,000 and (b) 50-μm radius and a *Q* of 19,000.

3. Modeling and analysis

3.1 Modeling observed interaction

To model these devices, we follow the analysis of Absil et al [25]. Assuming negligible depletion of the pump or signal due to the generation of the idler, the FWM conversion efficiency using an optical resonator is given by:

#92476 - $15.00 USD Received 4 Feb 2008; revised 19 Mar 2008; accepted 19 Mar 2008; published 26 Mar 2008
(C) 2008 OSA

$$\eta \equiv \frac{I_i^{(out)}}{I_s^{(in)}} = \left|\gamma P_p L_{eff}\right|^2 F_p{}^2 F_s F_i,$$

$$L_{eff}{}^2 = L^2 \exp(-\alpha L)\left|\frac{1-\exp(-\alpha L + j\Delta k L)}{\alpha L - j\Delta k L}\right|^2, \tag{1}$$

$$F_{p,s,i} = \left|\frac{\sigma}{1-\tau\exp(-\alpha L/2 + jk_{p,s,i}L)}\right|^2,$$

where $I_i^{(out)}$ is the output intensity of the idler, $I_s^{(in)}$ is the input intensity of the signal, the effective nonlinearity is given by $\gamma = (n_2\omega_0)/(cA_{eff})$, n_2 is the nonlinear index coefficient, ω_0 is the center frequency, c is the speed of light in vacuum, A_{eff} is the effective mode area, P_p is the input pump power, L_{eff} is the effective length, F_p, F_s, and F_i are the resonant intensity enhancement factors for the pump, signal and idler, respectively, L is the circumference of the ring, σ and τ are the coupling and transmission coefficients, respectively, with $|\sigma|^2 + |\tau|^2 = 1$, and $k_{p,s,i}$ are the wavenumbers of the pump, signal, and idler fields with the phase mismatch $\Delta k = 2k_p - k_s - k_i$. Although the modes of the microring resonator are inherently phase-matched [4], the non-zero value of the GVD causes the resonances to be unequally spaced in frequency (or energy). Since energy conservation must apply in parametric processes such as the FWM demonstrated in this experiment, the idler is not necessarily generated exactly at a cavity resonance. In our experiments, we operate closer to a doubly-resonant condition rather than a triply-resonant one since the GVD is far from zero, which reduces the intensity enhancement factor of our converted idler and therefore our maximum conversion efficiency. The term α represents the loss mechanisms in the system and includes both linear and nonlinear losses due to propagation loss, two-photon absorption (TPA) and free-carrier absorption (FCA) [28]. For the waveguide dimensions of our structures, we assume our free-carrier lifetime to be 500 ps [16]. We use the experimental values obtained for the propagation losses in the ring of 5 dB/cm and 7 dB/cm, the Q's of 19,000 and 23,000 for the 50-μm and 10-μm ring, respectively, n_2 = 6.5 x 10^{-14} cm^2/W, TPA value of 0.7 cm/GW [29-31] and D of 1600 ps/(nm·km) for the waveguides. Figure 3 shows excellent agreement between the above model and experiments, and we find that the conversion efficiency increases at low pump powers and then saturates. Furthermore, the reduction in power requirements and the conversion efficiency is accurately predicted by our model when comparing the smaller to the larger ring.

3.2 Modeling higher conversion efficiencies

Further increases approaching 0-dB conversion efficiency in the structures is possible by reducing the value of the GVD parameter (Fig. 4(a)) and simultaneously reducing the free-carrier lifetime (Fig. 4(b)). Using lower anomalous GVD values allows the intensity enhancement of the idler to increase, which results in a higher overall conversion efficiency. In Fig. 4(a), one can see that reducing the D value to 0 predicts a -13-dB conversion efficiency in a 5-μm radius ring with a free-carrier lifetime of 500 ps and 3 mW of input pump power. To simulate the potential improvement to the conversion efficiency by reducing the free-carrier lifetime, we no longer use the model described above. To accurately model increased conversion efficiencies, we simulate the interaction in the resonant path including depletion effects on the signal and reconversion of the idler back to the signal due to the FWM process. This model is now valid for conversion efficiencies greater than -10 dB but still assumes an undepleted pump. Our model predicts that reducing the free-carrier lifetime to 10 ps, for example, by integrating a diode-structure across the device and applying a reverse bias to sweep out the carriers [10, 32] allows for near-zero-dB conversion efficiency using 9 mW of

#92476 - $15.00 USD Received 4 Feb 2008; revised 19 Mar 2008; accepted 19 Mar 2008; published 26 Mar 2008
(C) 2008 OSA

input pump power in a 5-μm radius ring. Above a conversion of 0 dB inside the ring, parametric oscillation occurs and this adjusted model can no longer be applied.

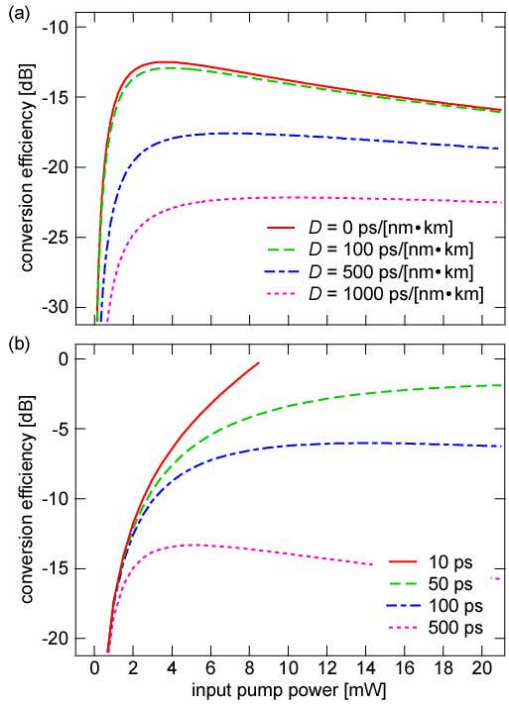

Fig. 4. Simulated dependence of conversion efficiency vs. power for a 5-μm radius ring on (a) GVD assuming a free carrier lifetime of 500 ps and (b) free carrier lifetime assuming GVD of 0 ps/(nm·km)

4. Conclusion

We have demonstrated wavelength conversion at ultra-low pump powers in micrometer-size photonic devices. This capability enables the integration of nonlinear optical components on-chip for all-optical functions such as wavelength conversion, signal regeneration, and switching. Conversion efficiencies close to 0 dB should be achievable by operating in a reverse-biased PIN device with waveguides exhibiting low anomalous GVD and could enable integrated silicon optical parametric oscillators and optical frequency combs. Demonstrations of this type of efficiency in a silicon CMOS-compatible photonic device in a practical, continuous-wave, low-power regime greatly enhances the possibility of an all-optical on-chip communication and signal-processing scheme with the potential of overcoming the current bandwidth limitations that plague CMOS electronics.

Acknowledgements

This work was funded by the Center for Nanoscale Systems, supported by the NSF and the New York State Office of Science, Technology and Academic Research. M.A.F. and A.L.G. also acknowledge support under the DARPA DSO Slow-Light Program. This work was performed in part at the Cornell NanoScale Facility, a member of the National Nanotechnology Infrastructure Network, which is supported by the National Science Foundation.

#92476 - $15.00 USD Received 4 Feb 2008; revised 19 Mar 2008; accepted 19 Mar 2008; published 26 Mar 2008

(C) 2008 OSA